JOURNAL OF AGRICULTURAL AND FOOD CHEMISTRY

pubs.acs.org/JAFC Article

Gypenoside LXXV Alleviates Colitis by Reprograming Macrophage Polarization via the Glucocorticoid Receptor Pathway

Wenjing Wu, Xian Qu, Chenxing Hu, Xuepeng Zhu, Mengqi Wan, Yifa Zhou,* and Hairong Cheng*

Cite This: https://doi.org/10.1021/acs.jafc.4c04784 Read Online

ACCESS | Metrics & More | Article Recommendations | Supporting Information

ABSTRACT: An imbalance in the macrophage phenotype is closely related to various inflammatory diseases. Here, we discovered that gypenoside LXXV (GP-75), a type of saponin from *Gynostemma pentaphyllum*, can reprogram M1-like macrophages into M2-like ones. On a mechanistic level, GP-75 inhibits NF-κB-COX2 signaling by targeting the glucocorticoid receptor (GR). Administration of GP-75, either orally or by intraperitoneal injection, significantly alleviates ulcerative colitis in mice, a pathogenesis associated with macrophage polarization. Clodronate liposomes, which deplete macrophages in mice, as well as GR antagonist RU486, abrogate the anticolitis effect of GP-75, thus confirming the pivotal role of macrophages in GP-75 function. We also showed that GP-75 has no toxicity in mice. Overall, this is the first report that demonstrates the effect of GP-75 on macrophage reprograming and as an agent against colitis. Because *G. pentaphyllum* is gaining popularity as a functional food, our findings offer new perspectives on the use of gypenosides as potential nutraceuticals for medical purposes.

KEYWORDS: *gypenoside LXXV, macrophage polarization, glucocorticoid receptor, colitis, toxicity*

1. INTRODUCTION

As crucial cells in the immune system, macrophages have the ability to differentiate into M1-like or M2-like phenotypes.[1] Although M1 macrophages can promote inflammation, M2 macrophages can inhibit inflammatory responses.[2,3] In this regard, macrophage polarization is associated with many inflammatory diseases. Hence, screening compounds that regulate macrophage polarization is highly significant for the development of new drugs to treat inflammatory diseases.[4−6] Ulcerative colitis (UC) is a chronic inflammatory bowel disease,[7] in which chemokines recruit monocytes to sites of inflammation and polarize macrophages into the M1-like state.[8] Compounds that reprogram macrophage polarization from M1-like to M2-like may provide an effective treatment for UC.[9,10]

Gynostemma pentaphyllum (Thunb.) Makino has long been used in China as a functional food and a dietary supplement. Products containing *G. pentaphyllum*, such as tea, instant powders, beverages, and sports drinks, are available internationally.[11,12] In addition, *G. pentaphyllum*, referred to as "Southern Ginseng", is well recognized for its pharmacological benefit, including in the treatment of ischemic stroke,[13] diabetes mellitus,[14] cancer,[15] atherosclerosis,[16] inflammation,[17] and hepatitis.[18] Gypenosides, a class of active substances in *G. pentaphyllum*, are the primary active agents in this species.[19] Gypenoside LXXV (GP-75) has been reported to contribute to wound healing,[20] prevent diabetic retinopathy,[21] and alleviate nonalcoholic steatohepatitis.[22] On a mechanistic level, GP-75 decreased the expression of TNF-α and IL-1β in hepatic macrophages.[22] However, the impact of GP-75 on macrophage polarization and colitis has yet to be investigated. This present study has discovered that GP-75 promotes M1- to M2-like macrophage polarization and prevents colitis in mice by targeting the glucocorticoid receptor (GR) and suppressing the NF-κB-COX2 signaling pathway without toxic side effects.

2. MATERIALS AND METHODS

2.1. Materials. GP-75 was prepared as previously reported (Hu et al., 2024). Sigma-Aldrich (St. Louis, MA) provided lipopolysaccharide (LPS). Fetal calf serum (FCS) was sourced from Sijiqing Bioengineering Material Co., Ltd. (Hangzhou, China). Enzyme-Linked Immunosorbent Assay (ELISA) Kit and antibiotics (penicillin and streptomycin) were purchased from Boster Biological Technology Co., Ltd. (Wuhan, China). KEL-R transfection reagent was acquired from Shanghai Juding Biotechnology Co., Ltd. (Shanghai, China). BD Biosciences (San Diego, CA) supplied β-Actin and F4/80. Antibodies, including ZO-1, Occludin, p-NF-κB, NF-κB, IκBα, CD206, and CD11c, were purchased from Cell Signaling Technology (Danvers, MA). Abcam (Massachusetts) supplied Claudin. The ELISA kit for Prostaglandin E2 (PGE2) was purchased from Shanghai Enzyme-linked Biotechnology Co., Ltd. (Shanghai, China). GR was provided by ABclonal Biotechnology in Wuhan, China. COX2 was purchased from Wuhan Servicebio Technology Co., Ltd. (Wuhan, China). Tanon (Shanghai, China) provided the ECL Western blotting reagent. Trypsin and phenyl methyl sulfonyl fluoride (PMSF) diluted in lysis buffer were purchased from Amersco (OH). Dextran sulfate sodium (DSS) was obtained from Yuanye Biotechnology Co. Ltd. (Shanghai, China).

2.2. Cell Culture. RAW264.7 cells were obtained from ATCC and cultured in Dulbecco's modified Eagle medium (DMEM) supplemented with 10% fetal calf serum (FCS) and 1% penicillin-

Received: May 31, 2024
Revised: August 24, 2024
Accepted: August 28, 2024

streptomycin. The cells were maintained in an incubator at 37 °C with 5% CO_2. The cells were plated in 24-well plates (20×10^4 cells/well) and treated with 100 ng/mL LPS and 50 or 100 μM GP-75 for 24 h.

2.3. Peritoneal Macrophages. Peritoneal macrophages were collected from mice in phosphate-buffered saline (PBS; 10 mL) and cultured in complete DMEM. Inflammation was induced in these cells by using 100 ng/mL LPS and 20 ng/mL IFNγ, and cells were cocultured with 100 μM of GP-75.

2.4. Quantitative Real-Time Polymerase Chain Reaction (qRT-PCR). The mRNA of cells and colon tissue was extracted by using TRIzol (TIANGEN, Beijing, China), and reverse-transcribed into cDNA using a FastKing One Step qRT-PCR Kit (TIANGEN, Beijing, China). Real-time PCR reactions were performed as previously reported. qRT-PCR was performed using a LightCycler 480 instrument (Roche). Primers are listed in Supporting Information Table S1.

2.5. Proteomic Analysis. Cell proteins were extracted for mass spectrometry. Protein quantification was assessed using a bicinchoninic acid protein kit. A total of 100 μg of protein was collected and reduced with 10 mM dithiothreitol at 37 °C for 1 h, followed by treatment with 20 mM iodoacetic acid (IAA, 25 °C for 1 h) to alkylate the proteins. After washing samples twice with 50 mM NH_4HCO_3, they were digested overnight at 37 °C using 1 mg trypsin (Promega, Wisconsin). Digested peptides were purified by using C18 tips (Minnesota Mining and Manufacturing Company, Minnesota), dried, and redissolved in 95% acetonitrile and 0.1% formic acid. Liquid chromatography elution was performed by using 0.1% formic acid. The mass spectrometer was a Q Exactive instrument (Thermo Fisher Scientific, Wilmington) operating in positive-ion mode. Following an initial MS scan, high collision dissociation was conducted on the 10 most dominant ions.

Proteome Discoverer software, version 2.2 (Thermo Fisher Scientific, Bremen, Germany) was used to analyze MS data, and proteins were matched against those in the mouse UniProt database with selection of differentially expressed proteins requiring a |log2 fold change| ≥ 2 and p-value < 0.05. Kyoto Encyclopedia of Genes and Genomes (KEGG) enrichment analysis was done online using the database OMIC SOLUTION (https://www.omicsolution.com/wkomics/passwd/KEGGEnrich/). The KEGG pathway was visualized at https://www.bioinformatics.com.cn.

2.6. ELISA Assay for PGE2 Detection. For this procedure, cells were exposed to 100 ng/mL LPS and 50 or 100 μM GP-75 for 24 h. The secretion level of PGE2 from the culture supernatant was measured by using an ELISA kit.

2.7. Western Blotting. Western blotting was carried out as previously reported.[23] Briefly, membranes were incubated overnight at 4 °C with the following primary antibodies: IκBα (9102 s, 1:1000), p-NF-κB (3033, 1:800), COX2 (GB15672, 1:1000), ZO-1 (ab190085, 1:1000), Claudin (ab211737, 1:1000), Occludin (91131s, 1:1000), and β-Actin (612656, 1:5000). After three washes with PBST, the poly(vinylidene difluoride) (PVDF) membranes were exposed to secondary antibodies and subsequently imaged.

2.8. Immunofluorescence Assay. RAW264.7 cells were treated for 15 min with 100 ng/mL LPS, and with or without 100 μM GP-75. Cells were then fixed in 4% polyformaldehyde (PFA) for 30 min and treated with an anti-NF-κB antibody (1:200) and incubated overnight at 4 °C, followed by washing with PBST. Cells were then treated with Hoechst reagent and secondary antibodies. Immunofluorescence microscopy was used to observe the location of NF-κB in the nucleus.

Colon tissues fixed in PFA were processed using a standard dehydration procedure and embedded in the OCT. Colon sections (5 μm) were cut from the OCT-embedded frozen blocks using a cryostatic microtome device (Leica, Wetzlar, Germany). Sections were then placed on microscope slides, washed with PBS, and incubated with FDB containing anti-F4/80, anti-CD11c, and anti-CD206 antibodies (1:100 dilution) for 12 h at 4 °C. Finally, sections were stained with Hoechst and secondary antibodies for 1 h.

2.9. Cell Transfection. Cells were transfected by using the protocol provided with the KEL-R transfection reagent. The GR-siRNA sequence was 5′-GCUGCUUCUCAGGCAGAUUTT-3′ and 5′-CCGGUUUAUUGCCAGGCAATT-3′. Briefly, cells were transfected with either GR-siRNA or Control-siRNA using the KEL-R transfection reagent. After a 24 h post-transfection incubation period, cells were treated with 100 ng/mL LPS alone or cocultured with 50 and 100 μM GP-75 for 15 min or 24 h. Western blotting was performed to assess the protein expression levels.

2.10. Molecular Modeling. The molecular structure of GP-75 was acquired by PubChem, and Schrödinger software LigPrep program was used to generate the three-dimensional structure. The crystal structure of GR-LBD was obtained from the Protein Data Bank (PDB code 4UDC). The structure was prepossesed using the Protein Preparation Wizard module available in the program Schrödinger. The most appropriate Enclosing box was selected using the Receptor Grid Generation program to precisely encircle the natural ligand structure and, consequently, to obtain the protein's active pocket. The docking score of GP-75 and GR-LBD was calculated using molecular docking and mechanics and the generalized Born surface area (MM-GBSA). Binding sites were visualized by using the PyMOL program.

2.11. Cellular Thermal Shift Assay (CETSA). Following exposure to dimethyl sulfoxide (DMSO) or 100 μM GP-75 for 24 h, RAW264.7 cells were collected in 1 mL of protein lysis solution that was then split into 8 parts. Samples underwent 3 cycles of heating at 48, 50, and 52 °C for 3 min each, followed by freezing in liquid nitrogen and thawing at room temperature. Proteins were collected for immunoblotting analysis.

2.12. Animals. Female C57BL/6J mice (20 ± 2 g), 6−8 weeks in age, were procured from Beijing Vital River Laboratory Animal Technology Co., Ltd. (Beijing, China). The mice were housed under standardized conditions. All animal experiments were performed in accordance with the NIH guidelines for the care and use of laboratory animals (NIH publication 85-23, revised 1996) and approved by the Animal Care and Use Committee of Northeast Normal University (SYXK 2018-0015).

2.13. Colitis Mouse Model. To induce colitis, the mice were treated with DSS (2.5% w/v) in drinking water for 7 days, followed by distilled water for 3 days. The mice in the control group were fed with equal amounts of water. For intraperitoneal injection of mice, GP-75 was dissolved in 5% DMSO in sterile PBS to different concentrations (1.25, 2.5, and 5 mg/kg). The control group and DSS group were intraperitoneally injected with 5% DMSO in sterile PBS. In the oral treatment experiment for colitis, GP-75 solutions at varying concentrations (2.5, 5, and 10 mg/kg, diluted in 0.5% CMC-Na solution) were administered orally once every 2 days. The control group and DSS group received the same diluted solution orally. Body weight, colon length, rectal bleeding, and diarrhea were scored. For macrophage depletion, mice received intraperitoneal injections of 200 μL of clodronate liposomes (Clo-lip) or PBS-liposomes (PBS-lip) (FormuMax Scientific, Inc.) on days −2, 1, 4, and 7. To antagonize GR, RU486 (20 mg/kg, dissolved in 0.1% DMSO diluted by corn oil, Sigma) was injected intraperitoneally on days −2, 0, 3, 6, and 9. The mice in the control group and DSS group were injected intraperitoneally vehicle (0.1% DMSO in corn oil), respectively.[24]

2.14. Flow Cytometry. Peritoneal cells were centrifuged at 1500 rpm for 10 min, and 100 μL of cells (5×10^6 cells/mL) were stained with F4/80 and CD11b, both diluted in PBS. For analysis on the flow cytometer, cells were washed twice with PBS and filtered through a 300-mesh nylon gauze.

2.15. Histological Analysis. Mice were sacrificed, and colon tissues were preserved in 4% PFA. Tissues were embedded in paraffin and microtome sectioned into 5 μm slices and stained with hematoxylin-eosin (HE). The histologic scores were evaluated as described in previous reports.[25]

2.16. Oral Toxicity of G75 *In Vivo*. After sacrificing mice, blood samples and the main organs (heart, liver, spleen, lung, and kidney) were collected. Renal function was assessed for blood samples based on blood urea nitrogen (BUN) and creatinine (Cr) levels. Hepatic function was evaluated by aspartate aminotransferase (AST) and alanine aminotransferase (ALT). The major organs were collected for further histopathological examination.

https://doi.org/10.1021/acs.jafc.4c04784
J. Agric. Food Chem. XXXX, XXX, XXX−XXX

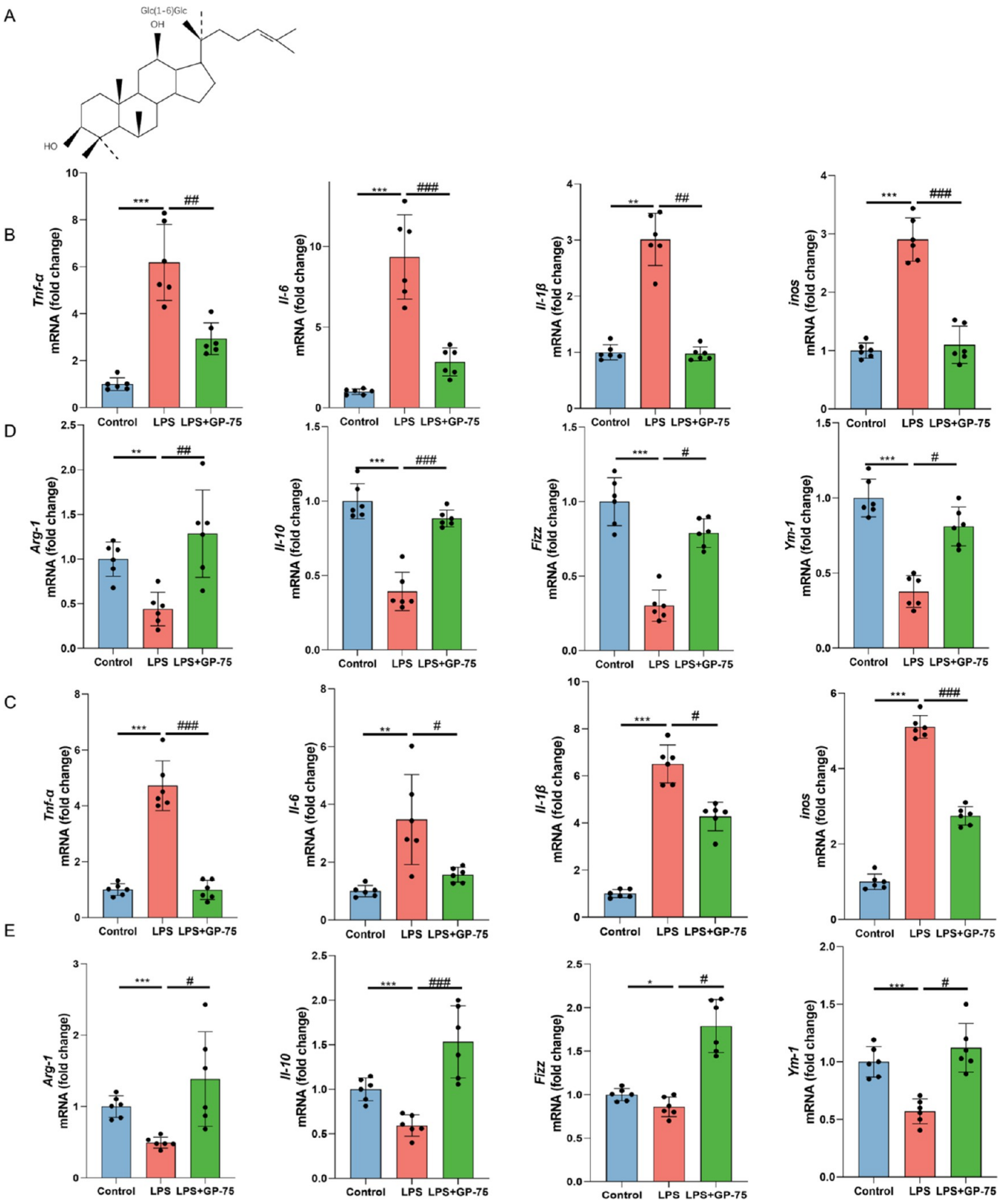

Figure 1. GP-75 regulated the polarization of macrophage *in vitro*. The chemical structure of GP-75 (A). Relative mRNA expression levels of M1 and M2 maker genes in RAW264.7 cells and peritoneal macrophages were normalized to expression of β-actin (B−E). Data are shown as the mean ± SD $^{*}p < 0.05$ and $^{**}p < 0.01$ compared to the Control group. $^{\#}p < 0.05$, $^{\#\#}p < 0.01$, and $^{\#\#\#}p < 0.001$ compared to the LPS group.

2.17. Acute Oral Toxicity Study. Forty mice (half males and half females) were randomly divided into two experimental groups: the control group and GP-75-treated group. The mice in the GP-75-treated group were given a single dose of GP-75 at the maximum feasible dose of 0.8 g/kg via gavage, whereas the control group was administered an equal volume of 0.5% (w/v) CMC-Na solution. The

https://doi.org/10.1021/acs.jafc.4c04784
J. Agric. Food Chem. XXXX, XXX, XXX−XXX

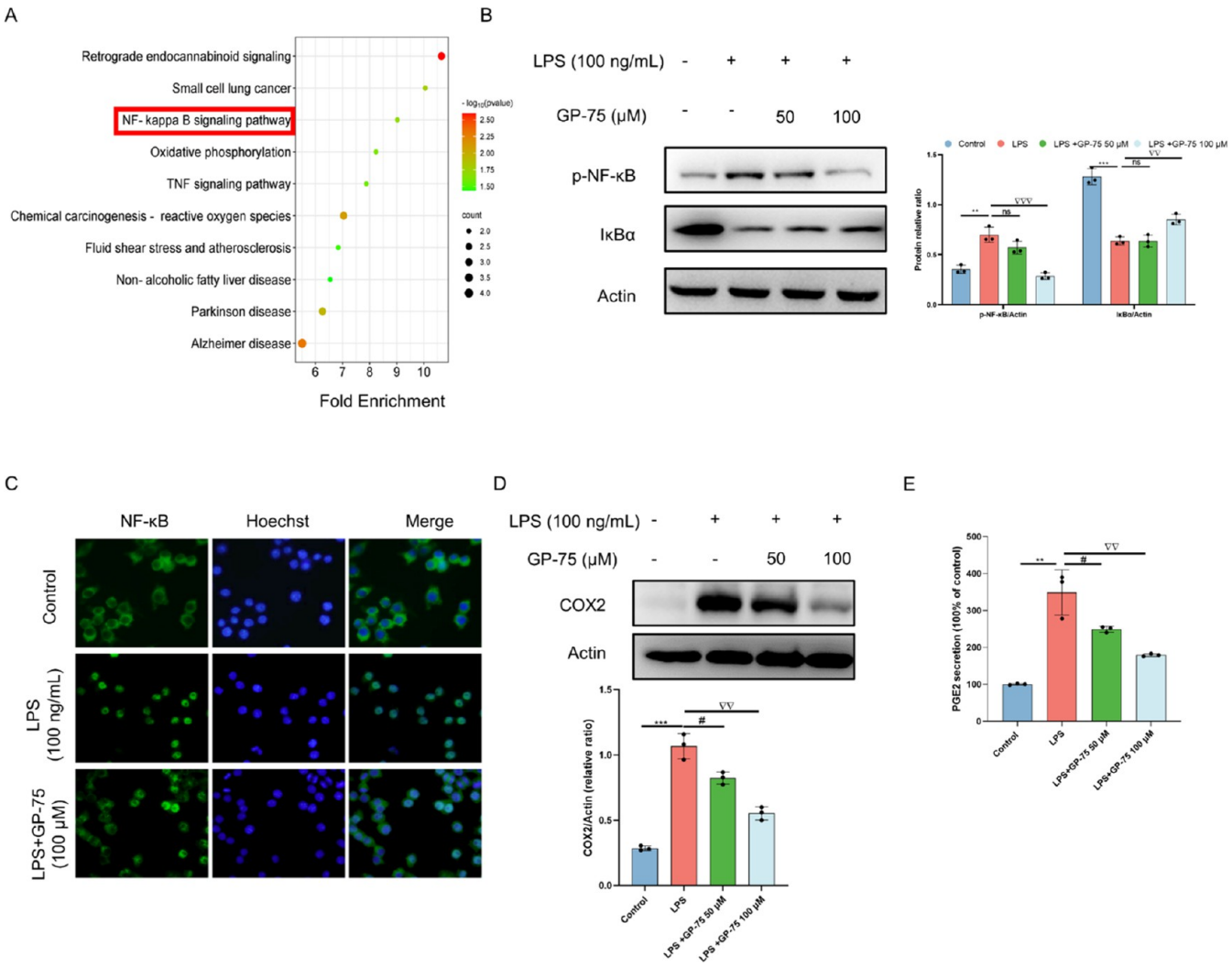

Figure 2. GP-75 suppresses the NF-κB-COX2 signaling pathway. Analysis of potential pathways influenced by GP-75 on macrophage polarization was conducted by using KEGG (A). Protein levels of p-NF-κB and IκBα in RAW264.7 cells (B). Nuclear translocation of NF-κB was determined by immunofluorescence (100× magnification) (C). Protein expression of COX2 was examined by Western blotting, and its activity was assessed by ELISA (D, E). Data are shown as the mean ± SD $^{**}p < 0.01$ and $^{***}p < 0.001$ compared to the control group. $^{\#}p < 0.05$, $^{\nabla\nabla}p < 0.01$ and $^{\nabla\nabla\nabla}p < 0.001$ compared to the LPS group.

body weight, food consumption, and mortality were recorded daily for 14 days.

2.18. Subacute Toxicity Experiment. Eighty mice (with an equal distribution of males and females) were randomly divided into four groups: a control group and three groups treated with different doses of GP-75. GP-75 at doses of (10, 20, and 50 mg/kg/day) were orally administrated for 28 days, whereas the control group was administered an equal volume of 0.5% (w/v) CMC-Na solution. Body weight was measured every week. The hematological analysis included red blood cell (RBC), platelet (PLT), white blood cell (WBC), lymphocyte (LYM), red blood cell volume (HCT), mean corpuscular volume (MCV), hemoglobin (HGB), and mean corpuscular hemoglobin concentration (MCHC). The biochemistry analysis including triglyceride (TG), total cholesterol (TC), aspartate aminotransferase (AST), alanine aminotransferase (ALT), alkaline phosphatase (ALP), creatinine (CRE), blood urea nitrogen (BUN), potassium (K^+), sodium (Na^+), chloride (Cl^-), total protein (TP), and albumin (ALB) were performed according to the instructions provided with kits (Nanjing Jiancheng Bioengineering Institute, Nanjing, Jiangsu, China). The organs were dissected and weighed. The organ coefficient of each animal was calculated as follows: Organ coefficient (%) = organ weight (g)/body weight (g) × 100%. The major organs were collected for further histopathological examination.

2.19. Statistical Analysis. Data are shown as the mean ± SD. Statistical significance between different groups was analyzed by using GraphPad Prism 8.0 software. The means of all data were compared by using the unpaired *t* test. $p < 0.05$ was considered statistically significant.

3. RESULTS

3.1. GP-75 Regulates Macrophage Polarization *In Vitro*. To investigate the influence of GP-75 (chemical structure shown in Figure 1A) on macrophage polarization, RAW264.7 cells and peritoneal macrophages were, respectively, induced with LPS to produce M1-like macrophages, and marker genes for M1-like and M2-like macrophages (*Tnf-α*, *Il-6*, *Il-1β*, *inos*, *Arg*-1, *Il-10*, *Fizz*, and *Ym*-1) were assessed by qRT-PCR. Compared to the LPS-treated group, GP-75 effectively inhibited the production of M1 macrophage-specific markers (*Tnf-α*, *Il-6 Il-1β*, and *inos*) (Figure 1B,D) and enhanced production of M2 macrophage-specific markers (*Arg-1*, *Il-10*, *Fizz*, and *Ym-1*) (Figure 1C,E). These results demonstrate that GP-75 can reprogram macrophages from M1-like to M2-like.

https://doi.org/10.1021/acs.jafc.4c04784
J. Agric. Food Chem. XXXX, XXX, XXX−XXX

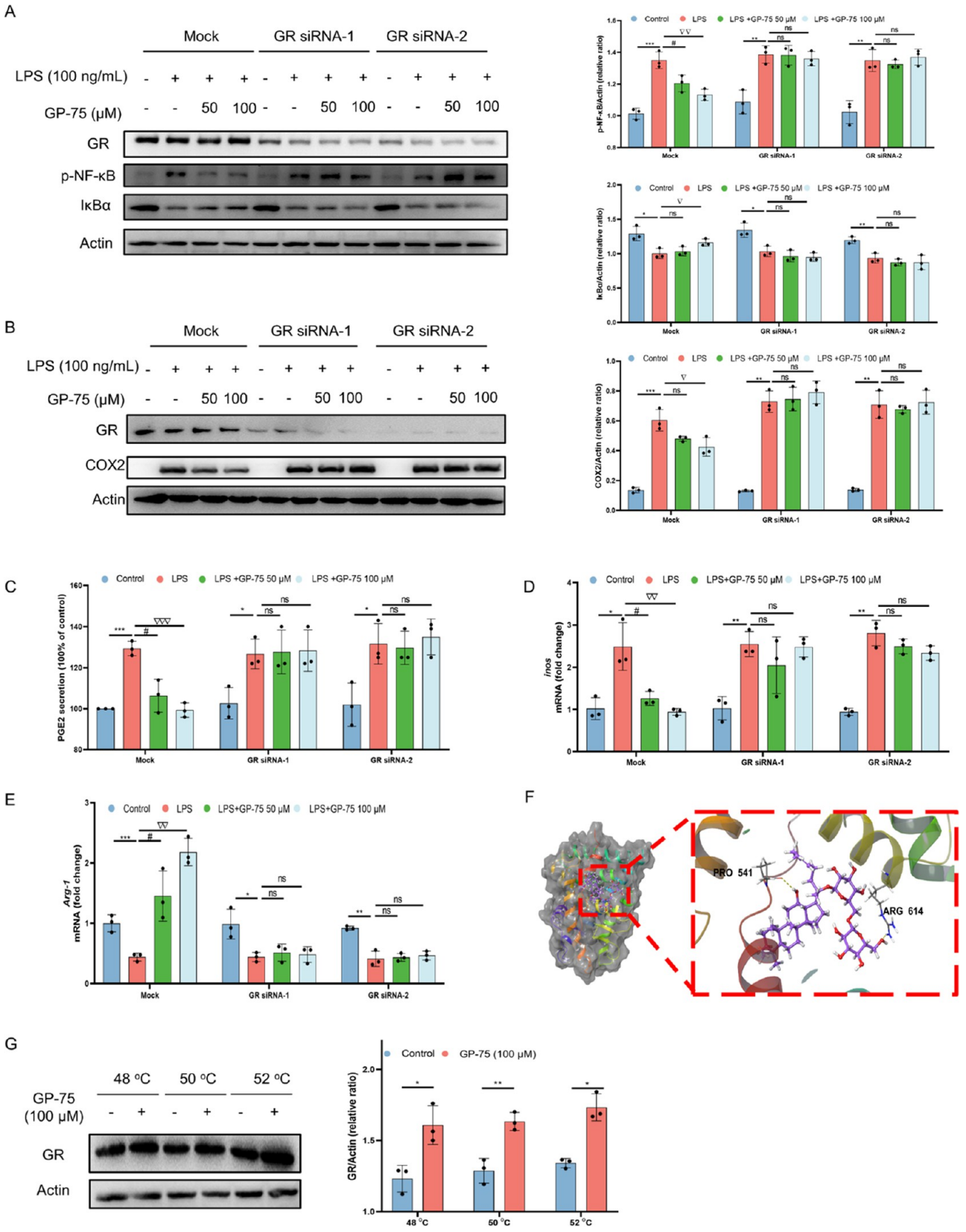

Figure 3. GP-75 inhibits NF-κB-COX2 signaling by targeting GR. Proteins in the NF-κB signaling pathways, COX2, and GR were assessed by Western blotting after GR was knocked down (A, B). Production of PGE2 was assessed by ELISA (C). Relative mRNA expression levels of *inos* and *Arg-1* (D, E). Molecular docking between GP-75 and GR using the GR crystal structure (PDB code 4UDC) (F). GR protein levels were evaluated by Western blotting after CETSA (G). Data are shown as the mean ± SD $^{*}p < 0.05$, $^{**}p < 0.01$ and $^{***}p < 0.001$ compared to the control group. $^{\#}p < 0.05$, $^{\nabla}p < 0.05$, $^{\nabla\nabla}p < 0.01$, and $^{\nabla\nabla\nabla}p < 0.001$ compared to the LPS group.

https://doi.org/10.1021/acs.jafc.4c04784
J. Agric. Food Chem. XXXX, XXX, XXX−XXX

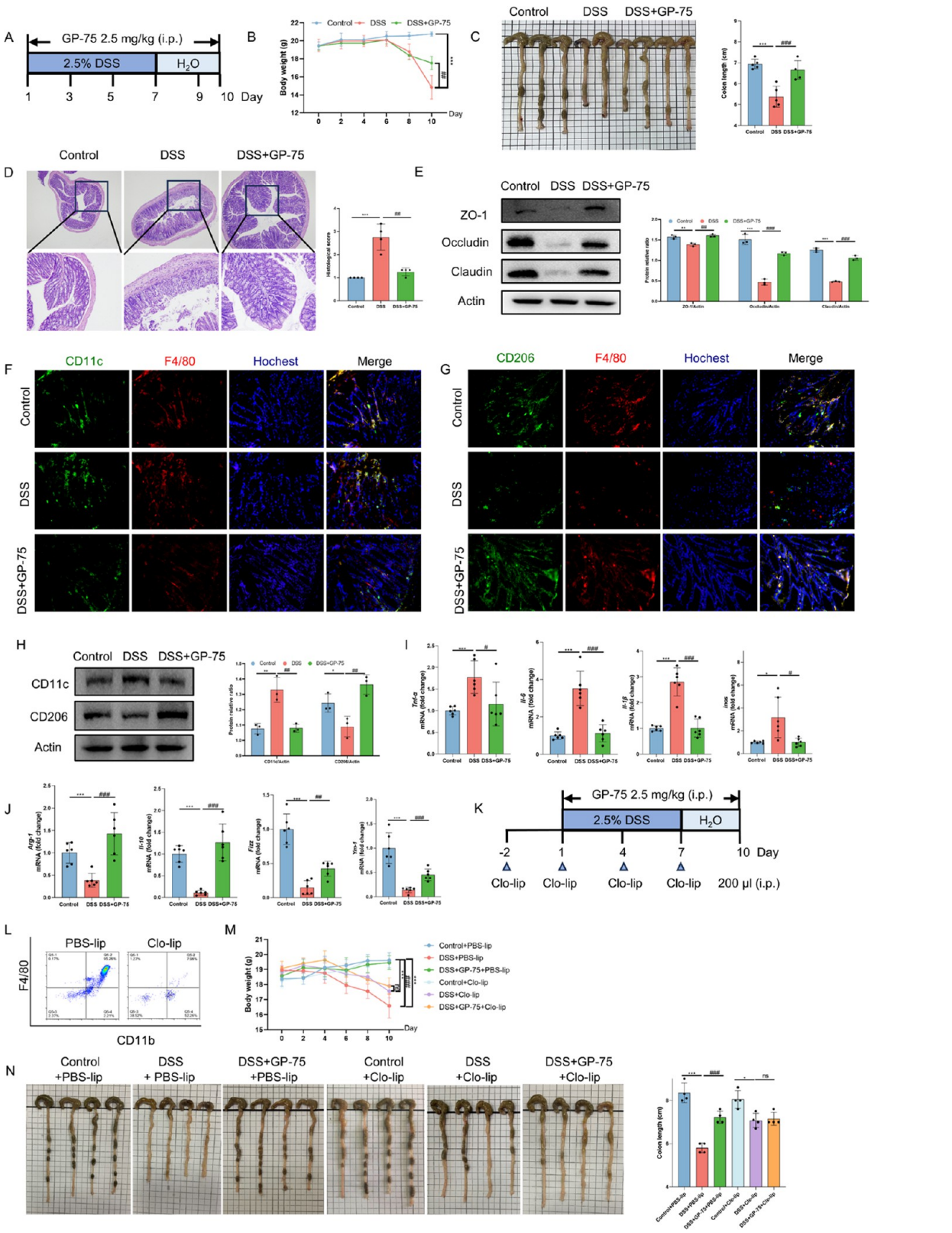

Figure 4. GP-75 prevents DSS-induced colitis by reprograming macrophage polarization. Schematic diagram of GP-75 in the treatment of colitis (A). Body weight (B), colon length (C). HE staining of colonic sections and histological score of colonic tissue (40× and 100× magnification) (D). Expression of ZO-1, Occludin, and Claudin was analyzed by Western blotting (E). F4/80 (red), CD11c (green), and CD206 (green) expression were assessed by immunofluorescence (100× magnification) (F, G). Protein levels of CD11c and CD206 in the colon (H). mRNA levels of indicated genes were analyzed by qRT-PCR (I, J). Schematic diagram of Clo-lip intraperitoneal injection (K). Flow cytometry for the number of macrophages in mice following Clo-lip treatment (L). Body weight (M), colon length (N). Data are shown as the mean ± SD for $n = 6$ or 4. $^{*}p < 0.05$, $^{**}p < 0.01$ and $^{***}p < 0.001$ compared with Control, Control + PBS-lip and Control + Clo-lip group. $^{\#}p < 0.05$, $^{\#\#}p < 0.01$ and $^{\#\#\#}p < 0.001$ compared with the DSS, DSS + PBS-lip and DSS + Clo-lip group.

https://doi.org/10.1021/acs.jafc.4c04784
J. Agric. Food Chem. XXXX, XXX, XXX−XXX

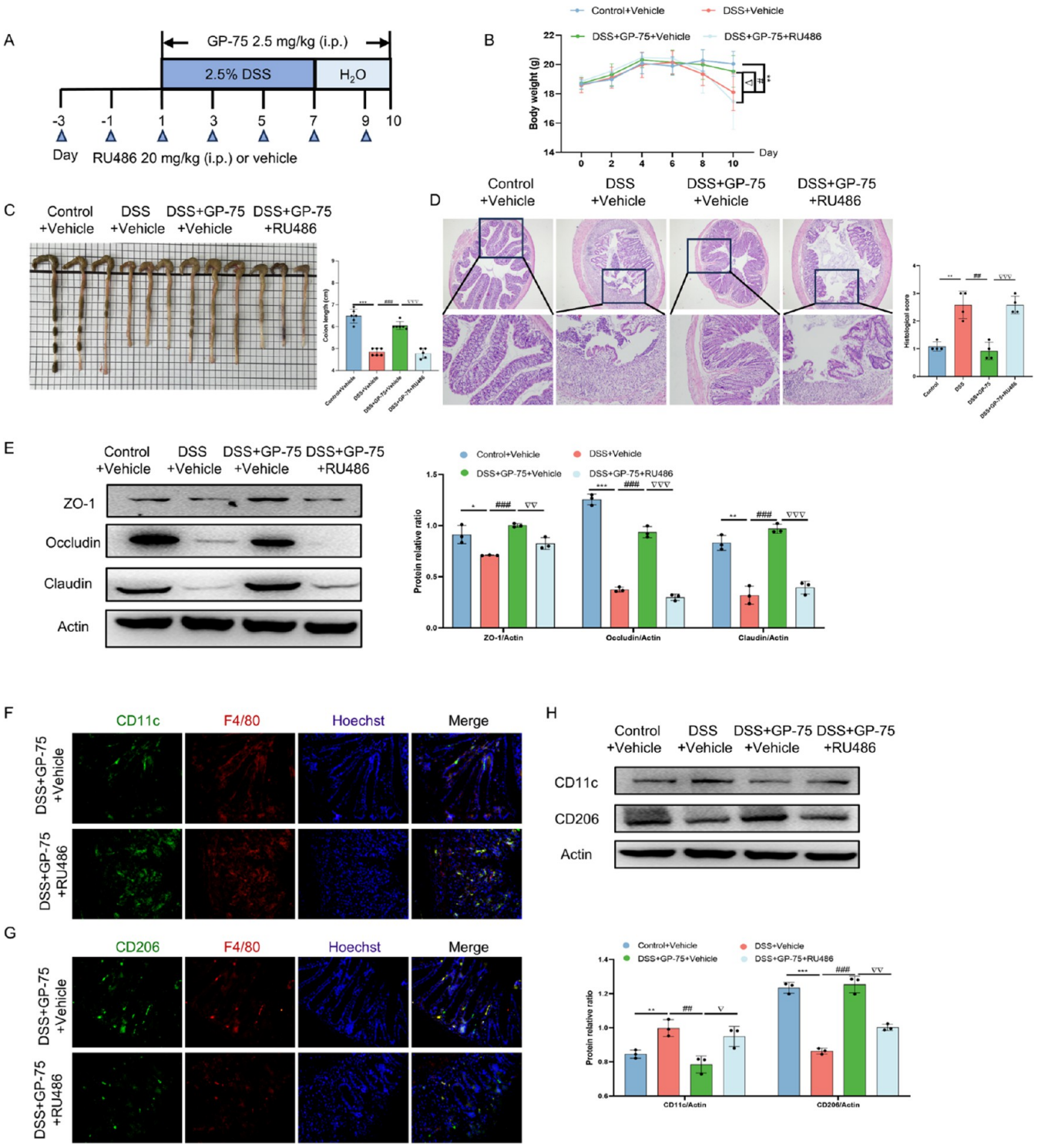

Figure 5. GP-75 ameliorates colitis via GR *in vivo*. Schematic diagram for the study (A). Body weight (B) and colon images, and colon length are shown (C). HE staining of colonic sections and histological score of colonic tissue (40× and 100× magnification) (D). Protein levels of ZO-1, Occludin, and Claudin were analyzed by Western blotting (E). F4/80 (red), CD11c (green), and CD206 (green) expression were assessed by immunofluorescence (100× magnification) (F, G). Protein levels of CD11c and CD206 were analyzed by Western blotting (H). Data are shown as the mean ± SD for $n = 8$. $^{*}p < 0.05$ and $^{**}p < 0.01$ compared to the Control + Vehicle group. $^{\#}p < 0.05$, $^{\#\#}p < 0.01$ and $^{\#\#\#}p < 0.001$ compared to the DSS+Vehicle group. $^{\nabla}p < 0.05$, $^{\nabla\nabla}p < 0.01$ and $^{\nabla\nabla\nabla}p < 0.01$ compared to the DSS + GP-75 + Vehicle group.

3.2. GP-75 Suppresses the NF-κB-COX2 Signaling Pathway. To investigate the molecular mechanism of GP-75 reprogramming of macrophage polarization, we performed proteomic analysis by mass spectrometry (Q Exactive, Thermo Fisher Scientific). We detected a total of 2224 proteins with 38 of them showing significant changes. KEGG analysis indicated that proteins in the NF-κB signaling pathway dominated (Figure 2A). To confirm the analysis, Western blotting was applied and demonstrated that GP-75 could robustly abrogate NF-κB phosphorylation and IkBα degradation (Figure 2B).

https://doi.org/10.1021/acs.jafc.4c04784
J. Agric. Food Chem. XXXX, XXX, XXX−XXX

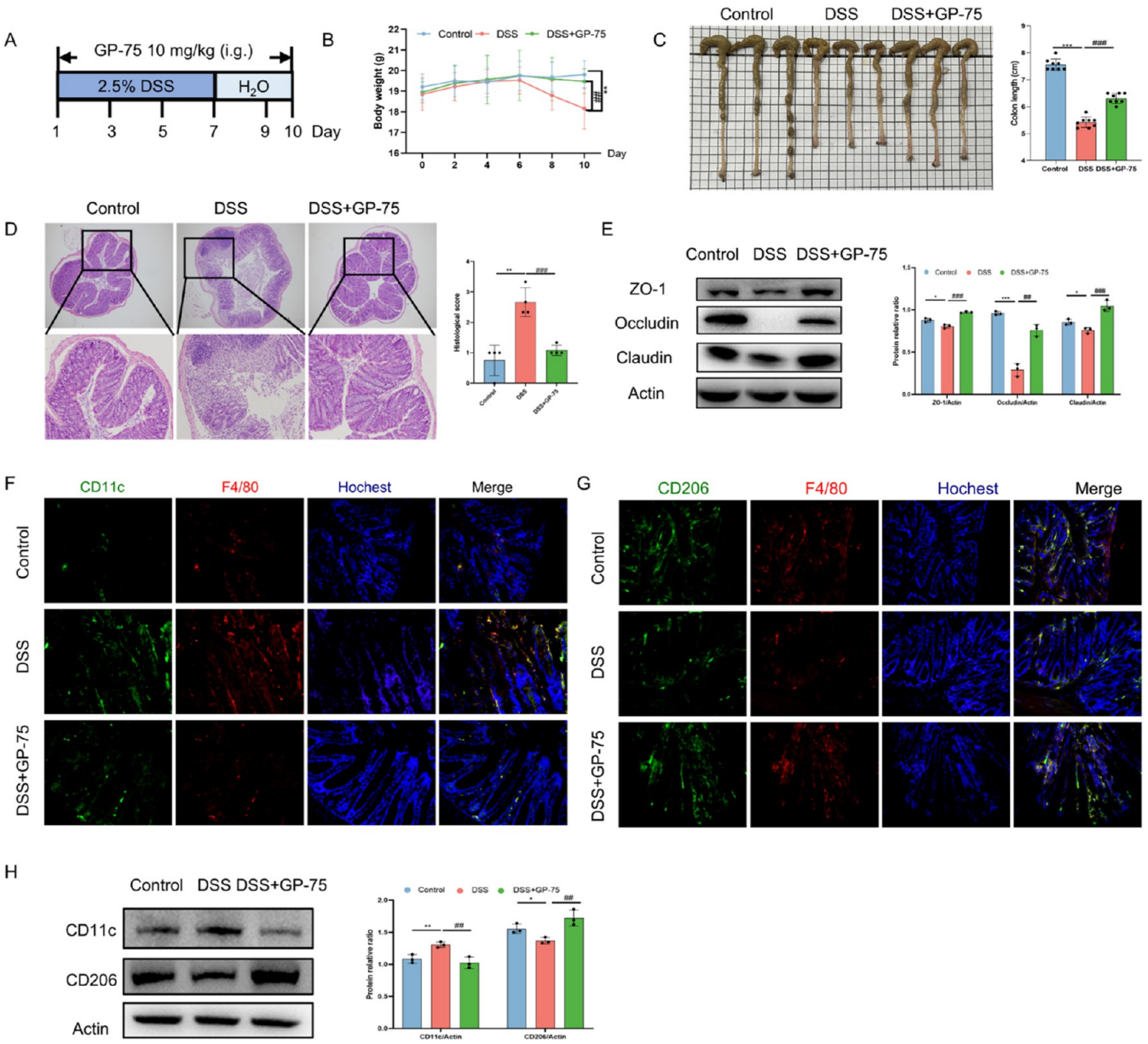

Figure 6. Oral administration of GP-75 prevents colitis. Schematic diagram for the present study (A). Body weight (B) and colon images, and colon length (C) are shown. HE staining of colonic sections and histological score of colonic tissue (40× and 100× magnification) (D). Protein levels of ZO-1, Occludin, and Claudin were analyzed by Western blotting (E). F4/80 (red), CD11c (green), or CD206 (green) expression was measured by immunofluorescence (100× magnification) (F, G). CD11c and CD206 expression was measured by Western blotting (H). Data are shown as the mean ± SD for $n = 6$. $^{*}p < 0.05$ and $^{**}p < 0.01$ compared to the control group. $^{\#}p < 0.05$, $^{\#\#}p < 0.01$ and $^{\#\#\#}p < 0.001$ compared to the DSS group. $^{\nabla\nabla}p < 0.01$ and $^{\nabla\nabla\nabla}p < 0.001$ compared to the DSS+GP-75 group.

Consistently, immunofluorescence showed that GP-75 clearly reduced the nuclear translocation of NF-κB (Figure 2C).

The KEGG analysis results also showed that the level of cyclooxygenase-2 (COX2) was changed robustly (Supporting Information Figure S1). COX2 is an enzyme that is largely responsible for the biochemical transformation of arachidonic acid to prostaglandin E2 (PGE2).[26] PGE2 can activate inflammasomes, suppress M2-like macrophage polarization, and trigger expression of key M1-like macrophage markers.[27] Therefore, we examined whether the effect of GP-75 might be related to the effect of COX2. Upon GP-75 treatment, the macrophages showed a robust decrease in COX2 expression (Figure 2D) and activity (Figure 2E). Because previous studies reported that NF-κB functions upstream of COX2,[28] we speculated that GP-75-mediated regulation of macrophage polarization likely occurs via suppressing NF-κB-COX2 signaling pathway.

3.3. GP-75 Is an Agonist of the Glucocorticoid Receptor (GR). In fibroblasts, GP-75 has been reported to promote wound healing by activating the GR,[20] and in inflammatory macrophages, GR activation can inhibit NF-κB phosphorylation.[29] Hence, the effect of GR on the effect of GP-75 was investigated in this study by using specific siRNAs. In GR-knockdown macrophages, GP-75 could not induce IκBα degradation or NF-κB phosphorylation (Figure 3A), nor could decrease COX2 protein expression or PGE2 secretion (Figure 3B,C). Consistently, the effect of GP-75 on macrophage polarization was diminished in GR-knockdown macro-

https://doi.org/10.1021/acs.jafc.4c04784
J. Agric. Food Chem. XXXX, XXX, XXX−XXX

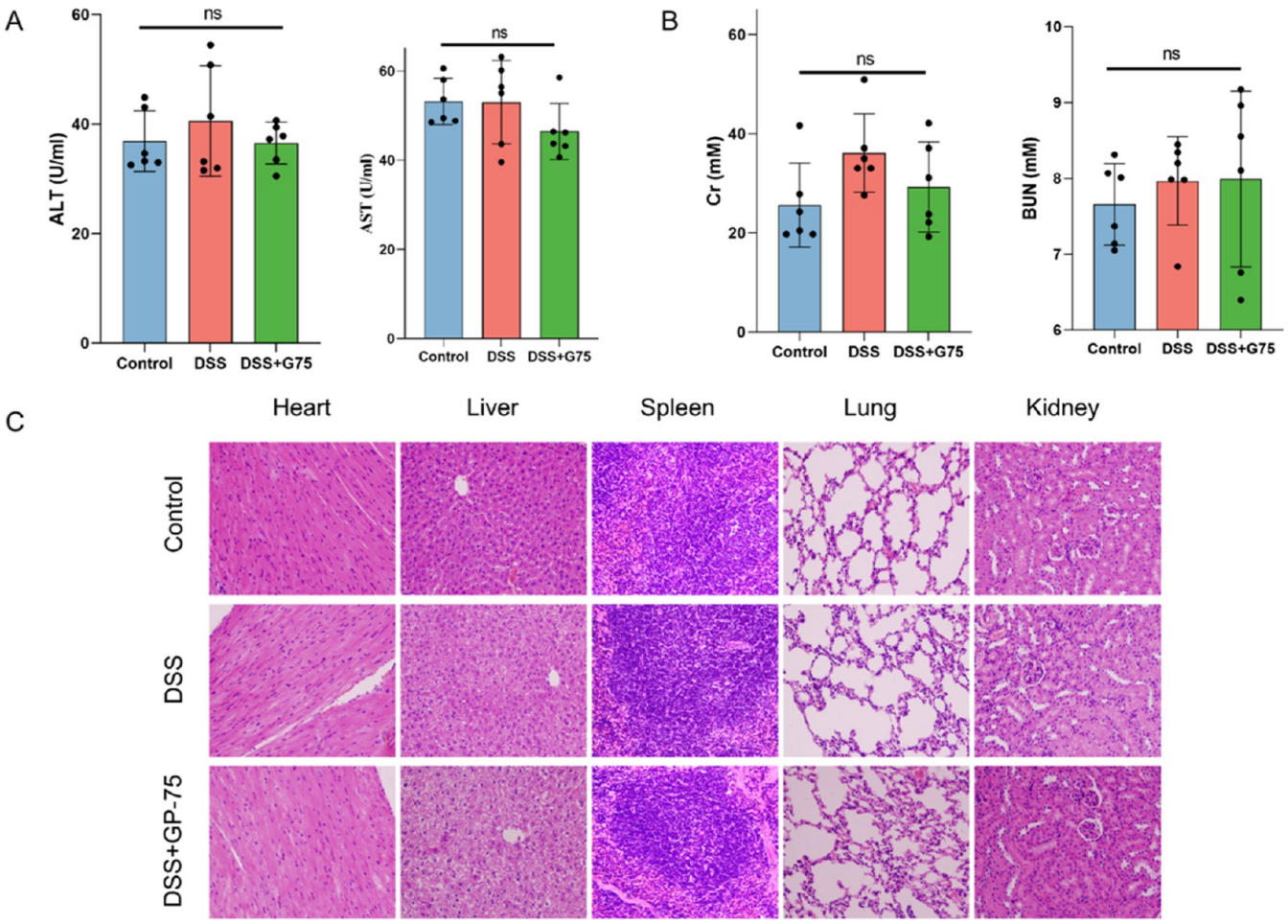

Figure 7. Oral toxicity of G75. Hepatic function was evaluated by ALT and AST levels (A). Renal function was assessed by BUN and Cr levels (B). HE staining of heart, liver, spleen, lung, and kidney excised from mice after different treatments (200× magnification) (C). Data are represented as mean ± SD for $n = 6$.

Table 1. Hematological Parameters of Mice in Different Treatment Groups[a]

	control group (0.5% CMC-Na)	GP-75 (10 mg/kg/day)	GP-75 (20 mg/kg/day)	GP-75 (50 mg/kg/day)
RBC ($\times 10^{12}$/L)	9.23 ± 56	9.36 ± 0.47	9.20 ± 0.53	9.21 ± 0.60**
PLT ($\times 10^{11}$/L)	9.84 ± 1.06	9.88 ± 0.73	10.03 ± 0.93	9.68 ± 0.52
WBC ($\times 10^{9}$/L)	12.67 ± 3.31	10.00 ± 2.93	13.82 ± 1.12	11.57 ± 2.02
LYM ($\times 10^{9}$/L)	9.79 ± 3.01	10.64 ± 3.55	12.34 ± 1.45	11.44 ± 1.38
HCT (%)	48.45 ± 3.08	49.14 ± 2.18	47.85 ± 2.98	48.49 ± 3.01
MCV (%)	52.84 ± 0.79	52.60 ± 0.87	52.04 ± 0.87	50.37 ± 0.62
HGB (g/L)	147.90 ± 6.08	148.50 ± 5.76	146.00 ± 8.42	146.20 ± 6.94**
MCHC (g/L)	303.50 ± 11.12	301.80 ± 6.03	304.70 ± 4.24	301.50 ± 9.11

[a]Note: **$p < 0.01$ compared with the control group. Data are represented as mean ± SD for $n = 10$.

phages (Figure 3D,E). These results demonstrate that the effect of GP-75 in regulating macrophage polarization is related to the GR.

GR is a transcription factor that can be activated by binding to specific ligands.[30] To determine whether GP-75 is a ligand of GR, we performed a molecular docking study that showed that GP-75 can bind to the surface of the active pocket of GR via hydrogen bonds with residues Pro541 and Arg614 (Figure 3F). The GP-75 binding affinity to GP was quite high, with an XP GScore of −5.122 kcal/mol and an MM/GBSA-based energy of −37.94 kcal/mol. Furthermore, the cellular thermal shift assay (CETSA) demonstrated the direct binding of GP-75 to GR, by virtue of the fact that GR exhibited higher thermal stabilization upon addition of GP-75 at temperatures of 48, 50, and 52 °C (Figure 3G). Taken together, these findings support the proposal that GP-75 is an agonist of GR in regulating macrophage polarization.

3.4. GP-75 Prevented DSS-Induced Colitis by Modulating Macrophage Polarization. To investigate whether GP-75 has an impact on macrophage polarization *in vivo*, we used the DSS-induced colitis murine model, a pathogenesis associated with macrophage polarization.[31] For this, mice were exposed to 2.5% DSS for 1 week, after which they received regular drinking water for 3 days (Figure 4A). GP-75 was administered intraperitoneally to mice at doses of 1.25, 2.5, and 5 mg/kg once every 2 days for 10 consecutive days.

https://doi.org/10.1021/acs.jafc.4c04784
J. Agric. Food Chem. XXXX, XXX, XXX−XXX

Table 2. Organ Coefficients of Mice Orally Administrated with Different Doses of Ginsenoside GP-75 for 28 Days[a]

	control group (0.5% CMC-Na)	GP-75 (10 mg/kg/day)	GP-75 (20 mg/kg/day)	GP-75 (50 mg/kg/day)
		male		
heart	0.71 ± 0.07	0.71 ± 0.10	0.77 ± 0.11	0.72 ± 0.07
liver	6.52 ± 0.90	6.37 ± 0.84	6.77 ± 1.07	7.05 ± 0.54
spleen	0.32 ± 0.05	0.30 ± 0.05	0.35 ± 0.06	0.36 ± 0.02*
lung	0.91 ± 0.11	0.91 ± 0.11	1.03 ± 0.13	0.92 ± 0.13
brain	2.37 ± 0.27	2.31 ± 0.21	2.51 ± 0.08	2.41 ± 0.17
kidney	1.74 ± 0.19	1.72 ± 0.16	1.90 ± 0.25	1.85 ± 0.13
pancreas	0.90 ± 0.14	0.98 ± 0.25	0.90 ± 0.27	1.03 ± 0.16
thymus	0.27 ± 0.06	0.26 ± 0.07	0.29 ± 0.06	0.30 ± 0.04
adrenal gland	0.05 ± 0.02	0.05 ± 0.00	0.05 ± 0.01	0.05 ± 0.02
testis	0.78 ± 0.08	0.78 ± 0.01	0.89 ± 0.12	0.83 ± 0.12
		female		
heart	0.72 ± 0.01	0.72 ± 0.06	0.73 ± 0.04	0.70 ± 0.10
liver	7.04 ± 0.79	6.91 ± 0.48	6.59 ± 0.41	6.38 ± 0.45*
spleen	0.42 ± 0.04	0.40 ± 0.03	0.44 ± 0.05	0.39 ± 0.02
lung	0.97 ± 0.09	0.88 ± 0.28	0.93 ± 0.08	0.95 ± 0.17
brain	2.44 ± 0.78	2.63 ± 0.08	2.67 ± 0.13	2.41 ± 0.35
kidney	1.76 ± 0.15	1.65 ± 0.13	1.67 ± 0.08	1.54 ± 0.02**
pancreas	1.10 ± 0.12	0.97 ± 0.14	1.07 ± 0.27	1.08 ± 0.18
thymus	0.40 ± 0.10	0.31 ± 0.07	0.38 ± 0.05	0.30 ± 0.06*
adrenal gland	0.04 ± 0.01	0.05 ± 0.02	0.05 ± 0.01	0.02 ± 0.01**
ovary + uterus	1.01 ± 0.18	0.82 ± 0.21	0.97 ± 0.15	0.93 ± 0.25

[a]Note: *$p < 0.05$ and **$p < 0.01$ compared with the control group. Data are represented as mean ± SD for $n = 10$.

Compared to the DSS group, GP-75 treatment at 2.5 or 5 mg/kg substantially restored body weight (Supporting Information Figure S2A) and colon length (Supporting Information Figure S2B). Therefore, we used the 2.5 mg/kg dose in subsequent studies. In addition to significantly restoring body weight (Figure 4B) and colon length (Figure 4C), GP-75 also significantly improved colonic tissue repair (Figure 4D) and increased the expression of tight junction proteins (Figure 4E).

We measured the infiltration of M1- and M2-like macrophages in the colon by immunofluorescence. Compared with the DSS group, GP-75 treatment clearly reduced the proportion of M1-like macrophages (Figure 4F), while simultaneously enhancing that of M2-like macrophages (Figure 4G). These results were further confirmed by Western blotting and qRT-PCR (Figure 4H−J). In addition, to evaluate whether macrophages are essential for GP-75 to alleviate DSS-induced colitis, clodronate-loaded liposomes (Clo-lip) and PBS-liposomes as vehicle control (PBS-lip) were intraperitoneally injected into mice (Figure 4K). The results showed that treatment with Clo-lip efficaciously depleted macrophages (Figure 4L). Upon depletion, GP-75 could not effectively protect mice from developing colitis, as evidenced by sustained body weight (Figure 4M) and colon length (Figure 4N). These findings confirmed that the anticolitis effect from GP-75 treatment is related to its reprograming effect of macrophage polarization.

3.5. GP-75 Ameliorates Colitis by Binding to GR. At the cellular level, GR activation plays an important role in GP-75-mediated macrophage polarization. To confirm the involvement of GR in the anticolitis property of GP-75 *in vivo*, we injected the GR inhibitor RU486 (20 mg/kg) or vehicle intraperitoneally in mice on days −2, 0, 3, 6, and 9 (Figure 5A), and RU486-treated mice showed minimal response to GP-75 as indicated by the lack of change in body weight (Figure 5B) or colon length (Figure 5C), as well as by histological examination (Figure 5D) and expression of tight junction proteins (Figure 5E). RU486 had no effect on mice of the control and DSS groups (data not shown). Consistently, GP-75-mediated regulation of macrophage polarization was also inhibited by GR inhibitor RU486 (Figure 5F−H). Reversal of the beneficial effects from GP-75 by treatment with RU486 further confirmed that GR plays an important role in the molecular mechanism of GP-75 in mediating macrophage polarization *in vivo*.

3.6. Oral Administration of GP-75 Also Reduced Colitis. Oral administration is advantageous, in terms of safety and compliance. Therefore, we investigated whether GP-75 could improve colitis when administered orally. For this study, GP-75 (2.5, 5, and 10 mg/kg) was administered orally to mice once every 2 days for 10 consecutive days (Supporting Information Figure S3). Our results showed that oral administration of GP-75 was administered at 10 mg/kg, which significantly reduced the signs of colitis as assessed by body weight (Figure 6B), colon shorting (Figure 6C), pathology (Figure 6D), and tight junction expression (Figure 6E). Oral administration of GP-75 also robustly modulated the polarization of macrophages from M1-like toward the M2-like (Figure 6F−H). These results indicated that the anticolitis effect of oral administration GP-75 was also closely related to its regulation of macrophage polarization.

3.7. Toxicity Test. Finally, we determined the safety of G75 for treating colitis. We analyzed blood samples and major organs after 10 days of treatment. The biochemical analysis of the blood demonstrated that two important indicators of liver function (ALT and AST) and two indicators of kidney function (Cr and BUN) were not affected upon oral gavage of 10 mg/kg G75 for 10 days (Figure 7A,B). Meanwhile, no anatomical changes were noted in the mice (Figure 7C). The results indicated that G75 had negligible toxicity in mice.

Moreover, acute and subacute oral toxicities of GP-75 have not been reported. To lay the foundation for its future applications, the safety of GP-75 was determined in the study.

https://doi.org/10.1021/acs.jafc.4c04784
J. Agric. Food Chem. XXXX, XXX, XXX−XXX

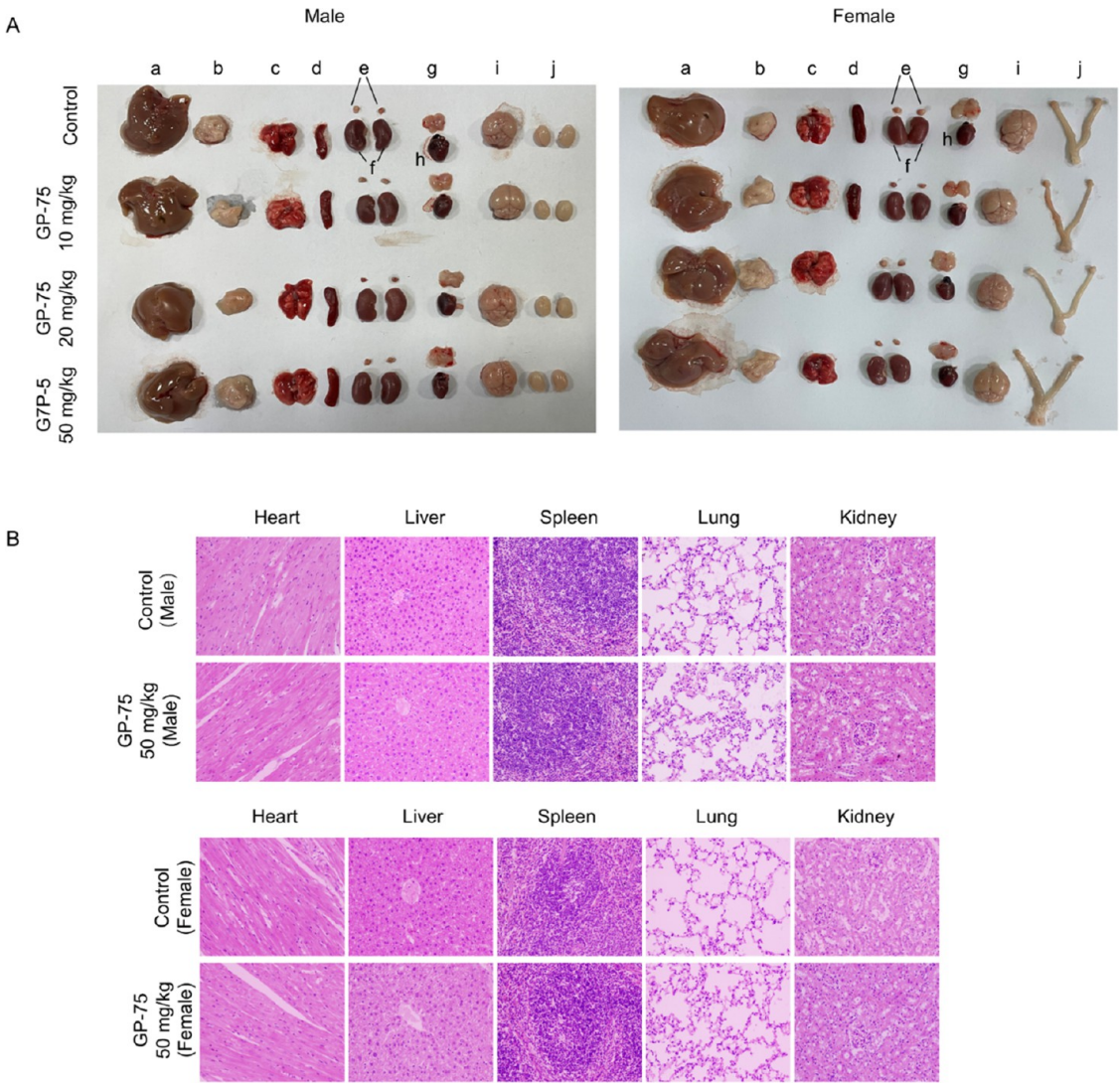

Figure 8. Acute and subacute oral toxicity of GP-75. Necropsy findings of mice (a, liver; b, pancreas; c, lung; d, spleen; e, adrenal gland; f, kidney; g, thymus; h, heart; i, brain; j, ovary of female mice; and k, testis of male mice) (A). HE staining of major organs in control and 50 mg/kg of GP-75 treatment groups (200× magnification) (B). Data are represented as mean ± SD for n = 10.

The limit test method was employed to determine the acute oral toxicity of GP-75, with a maximum feasible dose set at 0.8 g/kg. All mice survived, and no toxicity signs were observed. GP-75 treatment had no effect on body weight or food intake (Supporting Information Figure S4). No anatomical alterations were observed in any mice on day 14.

In the subacute oral toxicity experiment, the mice were divided into the control group and 10, 20, and 50 mg/kg GP-75 treatment group, respectively. All mice survived this experiment. As shown in Supporting Information Table S2, various dosages of GP-75 treatment had no impact on body weight of mice.

Table 1 displays the results of the hematological analysis. In comparison to the control group, 10 and 20 mg/kg doses of GP-75 had no effect on the values of RBC, PLT, WBC, LYM, HCT, MCV, HGB, and MCHC. The values of RBC and HGB were significantly reduced in the 50 mg/kg dose group, while the remaining indicators showed no significant differences. However, the changes of RBC and HGB levels were within the range of normal references.[32,33]

The biochemistry analysis including TG, TC, AST, ALT, ALP, CRE, BUN, K^+, Na^+, Cl^-, TP, and ALB are shown in Supporting Information Table S3. In comparison to the Control group, there was no significant difference in the blood biochemical parameters of mice when they were treated with various dosages of GP-75.

In addition, there were no significant changes in the organ coefficients of the heart, liver, spleen, lung, brain, kidney, pancreas, thymus, adrenal gland, testis, ovary, or uterus at doses of 10 and 20 mg/kg (Table 2). The coefficient of spleen was markedly reduced in male mice, and the coefficients of liver, kidney, thymus, and adrenal gland were significantly reduced in female mice at the dose of 50 mg/kg (Table 2). However, all measures remained within the normal range.[34] No lesions were observed in any of the examined organs (Figure 8A). Additionally, no signs of inflammation or tissue necrosis were observed in heart, liver, spleen, lung, or kidney in 50 mg/kg GP-75 treatment group (Figure 8B). Collectively, these results indicate that GP-75 have no toxicity when administered orally.

https://doi.org/10.1021/acs.jafc.4c04784
J. Agric. Food Chem. XXXX, XXX, XXX−XXX

4. DISCUSSION

In the past, *G. pentaphyllum* has been used as a functional food and dietary supplement to prevent or treat inflammation, hyperlipidemia, and liver diseases.[35−37] Gypenosides are the primary active agents in *G. pentaphyllum*.[38−40] Previous studies indicated that various gypenosides could exhibit anti-inflammatory effects. For example, gypenoside XIV reduces mRNA levels of IL-6, IL-1β, and TNF-α in LPS-stimulated BV-2 cells,[41] and gypenoside IX inhibits secretion of NO and IL-6 in rat C6 glial cells induced by LPS or TNF-α.[42] Similarly, gypenoside XVII decreases the production of IL-6 and TNF-α induced by LPS in RAW264.7 cells,[43] and also increases protein levels of CD206 and Arg-1 in oxidized-LDL stimulated THP-1 cells that indicates its role in regulating macrophage polarization.[39] To date, however, there have been no reports of GP-75 regulating macrophage polarization.

In the present study, our findings do demonstrate that gypenoside GP-75 reprograms macrophage polarization by modulating the NF-κB-COX2 signaling pathway. Previously, GP-75 has been shown to suppress nuclear translocation of NF-κB in oxygen-glucose deprived−reoxygenated H9c2 cells,[44] and yet it is not the only gypenoside to do so. For example, gypenoside XLIX reduces NF-κB phosphorylation in a cisplatin-treated human kidney tubular epithelial cell line,[45] and significantly decreases NF-κB levels in LPS-stimulated RAW264.7 cells.[46,47] In addition, gypenoside XIV has been shown to inhibit NF-κB activation in LPS-stimulated BV-2 cells,[41] and gypenoside IX deactivates NF-κB signaling in rat C6 glial cells induced by LPS and TNF-α[42] and inhibits phosphorylation of NF-κB in C8 cells.[48] Furthermore, gypenosides from the tetraploid *G. pentaphyllum* can inhibit p-NF-κB and the translocation of NF-κB in LPS-stimulated RAW264.7 cells.[49−51] Based on our research, as well as that from other laboratories, we can conclude that the NF-κB signaling pathway plays a pivotal role in mediating anti-inflammatory effects of gypenosides in general.

In terms of the glucocorticoid receptor pathway (GR), GP-75 has been shown to promote wound healing through the GR in fibroblasts.[20] Up until our present study, there had been no reports of GP-75 acting as an agonist of GR to regulate macrophage polarization. Here, we discovered that GP-75 indeed is a GR agonist that acts to reprogram macrophage polarization. Glucocorticoids (GCs), the ligands of GR, are pivotal in the treatment of many inflammatory diseases. Nevertheless, prolonged treatment with GCs has systemic adverse effects,[52,53] whereas GP-75 shows no acute and subacute toxicity *in vivo*. This, in turn, underscores the potential use of GP-75 as a GR agonist.

Previous studies have found that gypenoside XVII induces inflammation in the mouse ear,[54] and gypenoside A attenuates airway inflammation in a murine asthma model,[55] whereas gypenoside XIV reduces depressive-like behavior in mice.[48] However, the preventive effect of monomer gypenoside on colitis has not been documented. In the present study, we discovered that GP-75 substantially attenuates weight loss, colon shortening, and colon damage and reduces tight junction protein expression in mice with colitis. Our results further showed that depleting macrophages using phosphate liposomes significantly abrogates the effect of GP-75, thus confirming the involvement of macrophages in the action of GP-75.

In summary, this is the first study demonstrating that GP-75 can reprogram M1-like macrophages into M2-like ones, thereby attenuating colitis *in vivo*. Mechanistically, the effect of GP-75 involves the NF-κB-COX2 signaling pathway by targeting GR. Additionally, GP-75 has no significant toxicity in acute and subacute tests. Overall, we have established a solid foundation for GP-75 being used as a potential therapeutic for regulating macrophage-polarization-related inflammatory diseases like colitis.

■ ASSOCIATED CONTENT

Supporting Information

The Supporting Information is available free of charge at https://pubs.acs.org/doi/10.1021/acs.jafc.4c04784.

Primers sequences for qRT-PCR, body weight and biochemistry changes in subacute oral toxicity test, expression of COX2 and Traf1 in cells, anticolitis effect of different concentrations of GP-75, and body weight and food intake in acute oral toxicity test (PDF)

■ AUTHOR INFORMATION

Corresponding Authors

Yifa Zhou − *Engineering Research Center of Glycoconjugates, Ministry of Education, Jilin Provincial Key Laboratory of Chemistry and Biology of Changbai Mountain Natural Drugs, School of Life Sciences, Northeast Normal University, Changchun 130024, China*; Email: zhouyf383@nenu.edu.cn

Hairong Cheng − *Engineering Research Center of Glycoconjugates, Ministry of Education, Jilin Provincial Key Laboratory of Chemistry and Biology of Changbai Mountain Natural Drugs, School of Life Sciences, Northeast Normal University, Changchun 130024, China*; orcid.org/0000-0002-1800-569X; Phone: +86 18943109919; Email: chenghr893@nenu.edu.cn; Fax: +86 043185098212

Authors

Wenjing Wu − *Engineering Research Center of Glycoconjugates, Ministry of Education, Jilin Provincial Key Laboratory of Chemistry and Biology of Changbai Mountain Natural Drugs, School of Life Sciences, Northeast Normal University, Changchun 130024, China*

Xian Qu − *Engineering Research Center of Glycoconjugates, Ministry of Education, Jilin Provincial Key Laboratory of Chemistry and Biology of Changbai Mountain Natural Drugs, School of Life Sciences, Northeast Normal University, Changchun 130024, China*

Chenxing Hu − *Engineering Research Center of Glycoconjugates, Ministry of Education, Jilin Provincial Key Laboratory of Chemistry and Biology of Changbai Mountain Natural Drugs, School of Life Sciences, Northeast Normal University, Changchun 130024, China*

Xuepeng Zhu − *Engineering Research Center of Glycoconjugates, Ministry of Education, Jilin Provincial Key Laboratory of Chemistry and Biology of Changbai Mountain Natural Drugs, School of Life Sciences, Northeast Normal University, Changchun 130024, China*

Mengqi Wan − *Engineering Research Center of Glycoconjugates, Ministry of Education, Jilin Provincial Key Laboratory of Chemistry and Biology of Changbai Mountain*

https://doi.org/10.1021/acs.jafc.4c04784
J. Agric. Food Chem. XXXX, XXX, XXX−XXX

Natural Drugs, School of Life Sciences, Northeast Normal University, Changchun 130024, China

Complete contact information is available at: https://pubs.acs.org/10.1021/acs.jafc.4c04784

Author Contributions

W.W.: Conceptualization, data curation, formal analysis, investigation, methodology, project administration, validation, visualization, writing—original draft, writing—review and editing. X.Q.: Data curation, formal analysis, software, validation, visualization. C.H.: Data curation, resource. M.W. and X.Z.: Data curation, software. Y.Z.: Writing—review and editing. H.C.: Conceptualization, funding acquisition, supervision, writing—review and editing.

Notes

The authors declare no competing financial interest.

■ ACKNOWLEDGMENTS

This work was supported by the National Natural Science Foundation of China (Grants 32471329) and the Scientific and Technologic Foundation of Jilin Province (no. 20220401105YY).

■ REFERENCES

(1) Chen, S.; Saeed, A.; Liu, Q.; Jiang, Q.; Xu, H.; Xiao, G. G.; Rao, L.; Duo, Y. Macrophages in immunoregulation and therapeutics. *Signal Transduction Targeted Ther.* **2023**, *8* (1), No. 207.

(2) Liu, T.; Wang, L.; Liang, P.; Wang, X.; Liu, Y.; Cai, J.; She, Y.; Wang, D.; Wang, Z.; Guo, Z.; Bates, S.; Xia, X.; Huang, J.; Cui, J. USP19 suppresses inflammation and promotes M2-like macrophage polarization by manipulating NLRP3 function via autophagy. *Cell. Mol. Immunol.* **2021**, *18* (10), 2431−2442.

(3) Wen, J. H.; Li, D. Y.; Liang, S.; Yang, C.; Tang, J. X.; Liu, H. F. Macrophage autophagy in macrophage polarization, chronic inflammation and organ fibrosis. *Front. Immunol.* **2022**, *13*, No. 946832.

(4) Murray, P. J.; Wynn, T. Protective and pathogenic functions of macrophage subsets. *Nat. Rev. Immunol.* **2011**, *11* (11), 723−737.

(5) Hirayama, D.; Iida, T.; Nakase, H. The Phagocytic Function of Macrophage-Enforcing Innate Immunity and Tissue Homeostasis. *Int. J. Mol. Sci.* **2018**, *19* (1), No. 92.

(6) Na, Y. R.; Stakenborg, M.; Seok, S.; Matteoli, G. Macrophages in intestinal inflammation and resolution: a potential therapeutic target in IBD. *Nat. Rev. Gastroenterol. Hepatol.* **2019**, *16* (9), 531−543.

(7) Hegarty, L. M.; Jones, G.-R.; Bain, C. C. Macrophages in intestinal homeostasis and inflammatory bowel disease. *Nat. Rev. Gastroenterol. Hepatol.* **2023**, *20* (8), 538−553.

(8) Yip, J. L.; Balasuriya, G.; Spencer, S.; Hill-Yardin, E. The Role of Intestinal Macrophages in Gastrointestinal Homeostasis: Heterogeneity and Implications in Disease. *Cell. Mol. Gastroenterol. Hepatol.* **2021**, *12* (5), 1701−1718.

(9) Liu, L.; Wu, Y.; Wang, B.; Jiang, Y.; Lin, L.; Li, X.; Yang, S. DA-DRD5 signaling controls colitis by regulating colonic M1/M2 macrophage polarization. *Cell Death Dis.* **2021**, *12* (6), No. 500.

(10) Huang, C.; Wang, J.; Liu, H.; Huang, R.; Yan, X.; Song, M.; Tan, G.; Zhi, F. Ketone body β-hydroxybutyrate ameliorates colitis by promoting M2 macrophage polarization through the STAT6-dependent signaling pathway. *BMC Med.* **2022**, *20* (1), No. 148.

(11) Ahmed, A.; Saleem, M. A.; Saeed, F.; Afzaal, M.; Imran, A.; Nadeem, M.; Ambreen, S.; Imran, M.; Hussain, M.; Al Jbawi, E. Gynostemma pentaphyllum an immortal herb with promising therapeutic potential: a comprehensive review on its phytochemistry and pharmacological perspective. *Int. J. Food Prop.* **2023**, *26* (1), 808−832.

(12) Ji, X.; Shen, Y.; Guo, X. Isolation, Structures, and Bioactivities of the Polysaccharides from Gynostemma pentaphyllum (Thunb.) Makino: A Review. *Biomed. Res. Int.* **2018**, *2018*, No. 6285134.

(13) Liu, Y.; Zhao, J.; Song, J.; Mao, H.; Tan, G.; Zhang, Y.; Liu, C. Mechanism of Gynostemmae Pentaphylli Herba in the treatment of ischemic stroke based on network pharmacology and molecular docking. *Am. J. Transl. Res.* **2023**, *15* (6), 4079−4089.

(14) Huyen, V. T. T.; Phan, D. V.; Thang, P.; Hoa, N. K.; Ostenson, C. G. Gynostemma pentaphyllum Tea Improves Insulin Sensitivity in Type 2 Diabetic Patients. *J. Nutr. Metab.* **2013**, *2013*, No. 765383.

(15) Liao, W.; Khan, I.; Huang, G.; Chen, S.; Liu, L.; Leong, W. K.; Li, X. A.; Wu, J.; Wendy Hsiao, W. L. Bifidobacterium animalis: the missing link for the cancer-preventive effect of Gynostemma pentaphyllum. *Gut Microbes* **2021**, *13* (1), No. 1847629.

(16) Gou, S.-H.; Liu, B.-J.; Han, X.-F.; Wang, L.; Zhong, C.; Liang, S.; Liu, H.; Qiang, Y.; Zhang, Y.; Ni, J.-M. Anti-atherosclerotic effect of Fermentum Rubrum and Gynostemma pentaphyllum mixture in high-fat emulsion- and vitamin D3-induced atherosclerotic rats. *J. Chin. Med. Assoc.* **2018**, *81* (5), 398−408.

(17) Lüthje, P.; Lokman, E. F.; Sandström, C.; Östenson, C.-G.; Brauner, A. Gynostemma pentaphyllum exhibits anti-inflammatory properties and modulates antimicrobial peptide expression in the urinary bladder. *J. Funct. Foods* **2015**, *17*, 283−292.

(18) Lin, C. C.; Huang, P. C.; Lin, J. M. Antioxidant and hepatoprotective effects of Anoectochilus formosanus and Gynostemma pentaphyllum. *Am. J. Chin. Med.* **2000**, *28* (1), 87−96.

(19) Xie, P.; Luo, H. T.; Pei, W. J.; Xiao, M. Y.; Li, F. F.; Gu, Y. L.; Piao, X. L. Saponins derived from Gynostemma pentaphyllum regulate triglyceride and cholesterol metabolism and the mechanisms: A review. *J. Ethnopharmacol.* **2024**, *319* (Pt 1), No. 117186.

(20) Park, S.; Ko, E.; Lee, J. H.; Song, Y.; Cui, C. H.; Hou, J.; Jeon, B. M.; Kim, H. S.; Kim, S. C. Gypenoside LXXV Promotes Cutaneous Wound Healing In Vivo by Enhancing Connective Tissue Growth Factor Levels Via the Glucocorticoid Receptor Pathway. *Molecules* **2019**, *24*, No. 1595.

(21) Kim, D. Y.; Lee, K. W.; Kim, J.-H. Protective effect of gypenoside LXXV from Gynostemma pentaphyllum against oxidative stress-induced retinal degeneration in vitro and in vivo. *Phytomedicine Plus* **2021**, *1* (3), No. 100050.

(22) Lee, J. H.; Oh, J. Y.; Kim, S. H.; Oh, I. J.; Lee, Y.-h.; Lee, K. W.; Lee, W. H.; Kim, J.-H. Pharmaceutical Efficacy of Gypenoside LXXV on Non-Alcoholic Steatohepatitis (NASH). *Biomolecules* **2020**, *10* (10), No. 1426.

(23) Meng, Y.; Qu, Y.; Wu, W.; Chen, L.; Sun, L.; Tai, G.; Zhou, Y.; Cheng, H. Galactan isolated from Cantharellus cibarius modulates antitumor immune response by converting tumor-associated macrophages toward M1-like phenotype. *Carbohydr. Polym.* **2019**, *226*, No. 115295.

(24) Gao, Y.; Chu, S.; Li, J.; Li, J.; Zhang, Z.; Xia, C.; Heng, Y.; Zhang, M.; Hu, J.; Wei, G.; Li, Y.; Chen, N. Anti-inflammatory function of ginsenoside Rg1 on alcoholic hepatitis through glucocorticoid receptor related nuclear factor-kappa B pathway. *J. Ethnopharmacol.* **2015**, *173*, 231−240.

(25) Wang, F.; Chen, Y.; Itagaki, K.; Zhu, B.; Lin, Y.; Song, H.; Wang, L.; Xiong, L.; Weng, Z.; Shen, X. Wheat Germ-Derived Peptide Alleviates Dextran Sulfate Sodium-Induced Colitis in Mice. *J. Agric. Food Chem.* **2023**, *71* (42), 15593−15603.

(26) Munir, A.; Khushal, A.; Saeed, K.; Sadiq, A.; Ullah, R.; Ali, G.; Ashraf, Z.; Ullah Mughal, E.; Saeed Jan, M.; Rashid, U.; Hussain, I.; Mumtaz, A. Synthesis, in-vitro, in-vivo anti-inflammatory activities and molecular docking studies of acyl and salicylic acid hydrazide derivatives. *Bioorg. Chem.* **2020**, *104*, No. 104168.

(27) Sheppe, A. E. F.; Kummari, E.; Walker, A.; Richards, A.; Hui, W. W.; Lee, J. H.; Mangum, L.; Borazjani, A.; Ross, M. K.; Edelmann, M. J. PGE2 Augments Inflammasome Activation and M1 Polarization in Macrophages Infected With Salmonella Typhimurium and Yersinia enterocolitica. *Front. Microbiol.* **2018**, *9*, No. 2447.

(28) Lim, J. W.; Kim, H.; Kim, K. H. Nuclear factor-kappaB regulates cyclooxygenase-2 expression and cell proliferation in human gastric cancer cells. *Lab. Invest.* **2001**, *81* (3), 349−360.

(29) Rhen, T.; Cidlowski, J. A. Antiinflammatory action of glucocorticoids–new mechanisms for old drugs. *N. Engl. J. Med.* **2005**, *353* (16), 1711−1723.

(30) Han, Y.-M.; Kim, M. S.; Jo, J.; Shin, D.; Kwon, S.-H.; Seo, J. B.; Kang, D.; Lee, B. D.; Ryu, H.; Hwang, E. M.; Kim, J.-M.; Patel, P. D.; Lyons, D. M.; Schatzberg, A. F.; Her, S. Decoding the temporal nature of brain GR activity in the NFκB signal transition leading to depressive-like behavior. *Mol. Psychiatry* **2021**, *26* (9), 5087−5096.

(31) Zhao, X.; Di, Q.; Liu, H.; Quan, J.; Ling, J.; Zhao, Z.; Xiao, Y.; Wu, H.; Wu, Z.; Song, W.; An, H.; Chen, W. MEF2C promotes M1 macrophage polarization and Th1 responses. *Cell. Mol. Immunol.* **2022**, *19* (4), 540−553.

(32) Raabe, B. M.; Artwohl, J. E.; Purcell, J. E.; Lovaglio, J.; Fortman, J. D. Effects of weekly blood collection in C57BL/6 mice. *J. Am. Assoc. Lab. Anim. Sci.* **2011**, *50* (5), 680−685.

(33) Silva-Santana, G.; Bax, J. C.; Fernandes, D. C. S.; Bacellar, D. T. L.; Hooper, C.; Dias, A.; Silva, C. B.; de Souza, A. M.; Ramos, S.; Santos, R. A.; Pinto, T. R.; Ramão, M. A.; Mattos-Guaraldi, A. L. Clinical hematological and biochemical parameters in Swiss, BALB/c, C57BL/6 and B6D2F1 Mus musculus. *Anim. Models Exp. Med.* **2020**, *3* (4), 304−315.

(34) Marxfeld, H. A.; Küttler, K.; Dammann, M.; Gröters, S.; van Ravenzwaay, B. Body and organ weight data in 28-day toxicological studies in two mouse strains. *Data Brief* **2019**, *27*, No. 104632.

(35) Ren, D.; Zhao, Y.; Zheng, Q.; Alim, A.; Yang, X. Immunomodulatory effects of an acidic polysaccharide fraction from herbal Gynostemma pentaphyllum tea in RAW264.7 cells. *Food Funct.* **2019**, *10* (4), 2186−2197.

(36) Dai, N.; Zhao, F. F.; Fang, M.; Pu, F. L.; Kong, L. Y.; Liu, J. P. Gynostemma pentaphyllum for dyslipidemia: A systematic review of randomized controlled trials. *Front. Pharmacol.* **2022**, *13*, No. 917521.

(37) Wang, C.; Wang, P.; Chen, W.; Bai, Y. Mechanisms of Gynostemma pentaphyllum against non-alcoholic fibre liver disease based on network pharmacology and molecular docking. *J. Cell. Mol. Med.* **2022**, *26* (13), 3760−3771.

(38) Li, X.; Liu, H.; Lv, C.; Du, J.; Lian, F.; Zhang, S.; Wang, Z.; Zeng, Y. Gypenoside-Induced Apoptosis via the PI3K/AKT/mTOR Signaling Pathway in Bladder Cancer. *Biomed. Res. Int.* **2022**, *2022*, No. 9304552.

(39) Deng, W. Y.; Zhou, C. L.; Zeng, M. Y. Gypenoside XVII inhibits ox-LDL-induced macrophage inflammatory responses and promotes cholesterol efflux through activating the miR-182−5p/HDAC9 signaling pathway. *J. Ethnopharmacol.* **2024**, *319* (Pt 1), No. 117070.

(40) Cheng, S. C.; Liou, C. J.; Wu, Y. X.; Yeh, K. W.; Chen, L. C.; Huang, W. C. Gypenoside XIII regulates lipid metabolism in HepG2 hepatocytes and ameliorates nonalcoholic steatohepatitis in mice. *Kaohsiung J. Med. Sci.* **2024**, *40* (3), 280−290.

(41) Geng, Y.; Yang, J.; Cheng, X.; Han, Y.; Yan, F.; Wang, C.; Jiang, X.; Meng, X.; Fan, M.; Zhao, M.; Zhu, L. A bioactive gypenoside (GP-14) alleviates neuroinflammation and blood brain barrier (BBB) disruption by inhibiting the NF-κB signaling pathway in a mouse high-altitude cerebral edema (HACE) model. *Int. Immunopharmacol.* **2022**, *107*, No. 108675.

(42) Wang, X.; Yang, L.; Yang, L.; Xing, F.; Yang, H.; Qin, L.; Lan, Y.; Wu, H.; Zhang, B.; Shi, H.; Lu, C.; Huang, F.; Wu, X.; Wang, Z. Gypenoside IX Suppresses p38 MAPK/Akt/NFκB Signaling Pathway Activation and Inflammatory Responses in Astrocytes Stimulated by Proinflammatory Mediators. *Inflammation* **2017**, *40* (6), 2137−2150.

(43) Zhou, K.; Zhang, Y.; Zhou, Y.; Xu, M.; Yu, S. Production of Gypenoside XVII from Ginsenoside Rb1 by Enzymatic Transformation and Their Anti-Inflammatory Activity In Vitro and In Vivo. *Molecules* **2023**, *28* (19), No. 7001.

(44) Yu, H.; Shi, L.; Qi, G.; Zhao, S.; Gao, Y.; Li, Y. Gypenoside Protects Cardiomyocytes against Ischemia-Reperfusion Injury via the Inhibition of Mitogen-Activated Protein Kinase Mediated Nuclear Factor Kappa B Pathway In Vitro and In Vivo. *Front. Pharmacol.* **2016**, *7*, No. 148.

(45) Yang, Q.; Zang, H. M.; Xing, T.; Zhang, S. F.; Li, C.; Zhang, Y.; Dong, Y. H.; Hu, X. W.; Yu, J. T.; Wen, J. G.; Jin, J.; Li, J.; Zhao, R.; Ma, T. T.; Meng, X. M. Gypenoside XLIX protects against acute kidney injury by suppressing IGFBP7/IGF1R-mediated programmed cell death and inflammation. *Phytomedicine* **2021**, *85*, No. 153541.

(46) Zhou, M.; Cao, Y.; Xie, S.; Xiang, Y.; Li, M.; Yang, H.; Dong, Z. Gypenoside XLIX alleviates acute liver injury: Emphasis on NF-κB/PPAR-α/NLRP3 pathways. *Int. Immunopharmacol.* **2024**, *131*, No. 111872.

(47) Gao, H.; Kang, N.; Hu, C.; Zhang, Z.; Xu, Q.; Liu, Y.; Yang, S. Ginsenoside Rb1 exerts anti-inflammatory effects in vitro and in vivo by modulating toll-like receptor 4 dimerization and NF-kB/MAPKs signaling pathways. *Phytomedicine* **2020**, *69*, No. 153197.

(48) Jiang, Y.; Cheng, X.; Zhao, M.; Zhao, T.; Zhang, M.; Shi, Z.; Yue, X.; Geng, Y.; Gao, J.; Wang, C.; Yang, J.; Zhu, L. Gypenoside-14 Reduces Depression via Downregulation of the Nuclear Factor Kappa B (NF-kB) Signaling Pathway on the Lipopolysaccharide (LPS)-Induced Depression Model. *Pharmaceuticals* **2023**, *16* (8), No. 1152.

(49) Xie, Z.; Huang, H.; Zhao, Y.; Shi, H.; Wang, S.; Wang, T.; Chen, P.; Yu, L. L. Chemical composition and anti-proliferative and anti-inflammatory effects of the leaf and whole-plant samples of diploid and tetraploid Gynostemma pentaphyllum (Thunb.) Makino. *Food Chem.* **2012**, *132*, 125−133, DOI: 10.1016/j.foodchem.2011.10.043.

(50) Wang, B.; Li, M.; Gao, H.; Sun, X.; Gao, B.; Zhang, Y.; Yu, L. Chemical composition of tetraploid Gynostemma pentaphyllum gypenosides and their suppression on inflammatory response by NF-κB/MAPKs/AP-1 signaling pathways. *Food Sci. Nutr.* **2020**, *8* (2), 1197−1207.

(51) Wong, W. Y.; Lee, M. M.; Chan, B. D.; Ma, V. W.; Zhang, W.; Yip, T. T.; Wong, W. T.; Tai, W. C. Gynostemma pentaphyllum saponins attenuate inflammation in vitro and in vivo by inhibition of NF-κB and STAT3 signaling. *Oncotarget* **2017**, *8* (50), 87401−87414.

(52) Fardet, L.; Flahault, A.; Kettaneh, A.; Tiev, K. P.; Généreau, T.; Tolédano, C.; Lebbé, C.; Cabane, J. Corticosteroid-induced clinical adverse events: frequency, risk factors and patient's opinion. *Br. J. Dermatol.* **2007**, *157* (1), 142−148.

(53) Sarnes, E.; Crofford, L.; Watson, M.; Dennis, G.; Kan, H.; Bass, D. Incidence and US costs of corticosteroid-associated adverse events: a systematic literature review. *Clin. Ther.* **2011**, *33* (10), 1413−1432.

(54) Yu, S.; Zhou, X.; Li, F.; Xu, C.; Zheng, F.; Li, J.; Zhao, H.; Dai, Y.; Liu, S.; Feng, Y. Microbial transformation of ginsenoside Rb1, Re and Rg1 and its contribution to the improved anti-inflammatory activity of ginseng. *Sci. Rep.* **2017**, *7* (1), No. 138.

(55) Huang, W. C.; Wu, S. J.; Yeh, K. W.; Liou, C. J. Gypenoside A from Gynostemma pentaphyllum Attenuates Airway Inflammation and Th2 Cell Activities in a Murine Asthma Model. *Int. J. Mol. Sci.* **2022**, *23* (14), No. 7699, DOI: 10.3390/ijms23147699.